Journal of Science with Technological Applications
Research Article

D. Rojas[1*], **O. Prat**[1], **J. P. Sanhueza**[1], **J. García**[2]

[1] *Departamento de Ingeniería de Materiales, Universidad de Concepción, Edmundo Larenas 270, Concepción, Chile*
[2] *Sandvik Tooling – R&D Materials and Processes, Lerkrogsvägen 19, SE-126 80, Stockholm, Sweden*

Corresponding author: davrojas@udec.cl

Graphical abstract

Design of steel alloys 10-12% Cr resistant to high temperatures by thermodynamic modeling

Abstract

This work aims to design 10-12%Cr creep resistant steels with tailor-made microstructures for applications in power plants and petrochemical components. A detailed study regarding the selection of the precipitates which enhance the creep resistant properties was carried out considering metallurgical principles. In addition, the effect and interaction of the alloying elements as well as the temperatures of the heat treatments were investigated by thermodynamic modelling. As main results two alloys were designed; Alloy 10.5CrWVNb with ferritic matrix, Nb-MX, V-MX, $M_{23}C_6$, Laves phase and Z-phase at 650 °C and alloy 10.5CrTiMo with ferritic matrix, Ti.MX, Nb-MX, $M_{23}C_6$ and Laves phase at 650 °C. Ti addition in alloy 10.5CrTiMo promotes the precipitation of fine disperse Ti carbonitrides which improve the creep resistance and effectively inhibit the precipitation of the Z-phase. On the other hand, Z-phase is expected to precipitate in alloy 10.5Cr WVNb. However, further studies must be carried out to clarify the precipitation kinetics of the Z-phase.

Keywords
Steels 10-12% Cr
Computational Modeling
Heat Resistant Steels
Design of Alloys

Diseño de aleaciones de acero 10-12%Cr resistentes a alta temperatura mediante modelado termodinámico

Resumen

Este trabajo tiene como objetivo diseñar aceros 10-12%Cr resistentes al creep. Estos aceros presentan una microestructura propicia para las altas exigencias de componentes para plantas de producción de energía y petroquímica. Se realizó un estudio detallado basado en principios metalúrgicos y modelado termodinámico, sobre los efectos e interacción de los elementos aleantes y de los tratamientos térmicos para mejorar la resistencia al creep. Como resultados, se diseñaron dos aleaciones; La aleación 10.5CrWVNb con matriz ferritica, Nb-MX, V-MX, $M_{23}C_6$, fase Laves y fase Z a 650 °C y la aleación 10.5CrTiMo con ferrita, Ti-MX, Nb-MX, $M_{23}C_6$, y fase Laves a 650 °C. El Ti en la aleación 10.5CrTiMo favorece la fina y dispersa precipitación de Ti(C,N), que mejora la resistencia al creep e inhibe eficazmente la precipitación de Z. En la aleación 10.5Cr WVNb, se espera la precipitación de la fase Z. Sin embargo, se requieren estudios adicionales para dilucidar la cinética de precipitación de esta fase.

Palabras claves
Aceros 10-12%Cr
Modelado Computacional
Aceros Resistentes al Calor
Diseño de Aleaciones

Recived: 08-09-2017
Accepted: 02-10-2017
Publishing date: 15 – Noviembre - 2017
Revision Code: 20170908-AAAA [Pag. 15-26]

Corresponding author:
davrojas@udec.cl

Journal of Science with Technological Applications
Research Article

Design of steel alloys 10-12% Cr resistant to high temperatures by thermodynamic modeling

D. Rojas[1*], **O. Prat**[1], **J. P. Sanhueza**[1], **J. García**[2]

[1] *Departamento de Ingeniería de Materiales, Universidad de Concepción, Edmundo Larenas 270, Concepción, Chile*
[2] *Sandvik Tooling – R&D Materials and Processes, Lerkrogsvägen 19, SE-126 80, Stockholm, Sweden*

Corresponding author: davrojas@udec.cl

Abstract

This work aims to design 10-12%Cr creep resistant steels with tailor-made microstructures for applications in power plants and petrochemical components. A detailed study regarding the selection of the precipitates which enhance the creep resistant properties was carried out considering metallurgical principles. In addition, the effect and interaction of the alloying elements as well as the temperatures of the heat treatments were investigated by thermodynamic modelling. As main results two alloys were designed; Alloy 10.5CrWVNb with ferritic matrix, Nb-MX, V-MX, $M_{23}C_6$, Laves phase and Z-phase at 650 °C and alloy 10.5CrTiMo with ferritic matrix, Ti.MX, Nb-MX, $M_{23}C_6$ and Laves phase at 650 °C. Ti addition in alloy 10.5CrTiMo promotes the precipitation of fine disperse Ti carbonitrides which improve the creep resistance and effectively inhibit the precipitation of the Z-phase. On the other hand, Z-phase is expected to precipitate in alloy 10.5Cr WVNb. However, further studies must be carried out to clarify the precipitation kinetics of the Z-phase.

Keywords
Steels 10-12% Cr
Computational Modeling
Heat Resistant Steels
Design of Alloys

1. Introduction

The Martensitic/Ferritics 9-12%Cr steel (all values are in wt. %) are key material for the construction of fossil fuel power plants and petrochemical industry, due to they offer the best combination of high creep strength, high resistance against thermal fatigue, high steam oxidation resistance, low cost and good manufacturability, operating in the creep range at temperatures up to 600 °C [1, 2]. Due to new environmental regulations, energy saving requirement and operational conditions, there is an increase in the service temperature up to 650 °C [3, 4]. The elevated working temperature and the exposure to stress during service promote micro-structural degradation, reflected in a sudden decrease on the creep strength [5]. Many attempts have been made in the last 10-15 years in order to develop strong martensitic 1012%Cr steels, but all of these steels have failed in long-term creep [6]. It now seems clear that the failure is mainly due to unexpected precipitation of coarse Z-phase (Cr(V, Nb)N nitrides), which dissolve the finely dispersed V and Nb rich MX nitrides, which are essential to creep strength [7]. Recent investigations have demonstrated that the Z-phase precipitation is strongly accelerated by high Cr contents in these steels [8, 9]. Newly developed steels containing 9-10%Cr and small additions of V, Nb and N, which generate strengthening by finely dispersed V and Nb rich MX nitrides, showed stable longterm creep behaviour up to 100.000 h at 600 °C [10]. The 9-

10%Cr steels have limited steam oxidation resistance, in order to increase the steam temperature above 600 °C a higher Cr content is mandatory for oxidation protection [11].
In this work two 10.5%Cr steels with tailor-made microstructure were design and produced considering applications for power plants and petrochemical components, in order to achieve high creep strength at 650 °C and 100 MPa. The alloy design was supported by thermodynamic calculations. ThermoCalc was used for calculations of the phase equilibria and the evaluation of phase stabilities, so that the influence of composition (addition of elements) and heat treatments on the multicomponent 10.5%Cr alloys could be modelled. Two lines of studied were considered. The first alloy 10.5CrWVNb was designed to study the microstructure regarding the phase precipitation and evolution, focused on the precipitation kinetic of the Z phase. The second alloy was design in order to avoid the precipitation of Z phase with balanced addition of Ti, C and N.

2. Experimental procedure

2.1 Thermodynamic modelling

The ThermoCalc software has been employed for the alloys design [12]. ThermoCalc is a powerful tool used to perform thermodynamic and phase diagram calculations for multi-component systems [12-14]. The software is based on the CALPAHD method, where all the thermodynamic information as Gibbs energy is stored in various databases. With this tool the influence of composition and heat treatments on the 10.5%Cr martensitic/ferritic steels was modelled. Upon modelling, the time and costs of trial-anderror of conventional alloy development can be reduced. All calculations were carried out with the ThermoCalc database TCFe7 [12].

2.2 Alloy production

Two alloys were prepared by vacuum induction melting (Fig. 1 to 3) with masses of about 9 kg.
The samples were hot-rolled, austenitised and tempered with following parameters:

- Hot-rolling at 1200°C with posterior air cooling (60% section reduction). The process and the final samples are shown in Fig. 4 and 5.
- Austenisation heat treatment for 0.5 h at 1100°C

Figure 1. Vacuum induction furnace.

Figure 2. Charged crucible.

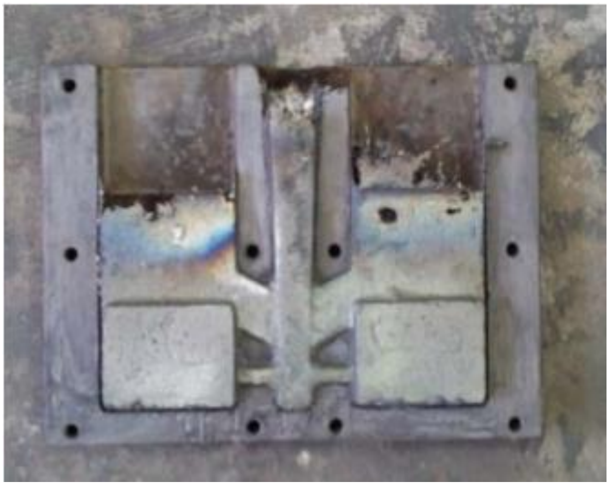

Figure 3. Mold.

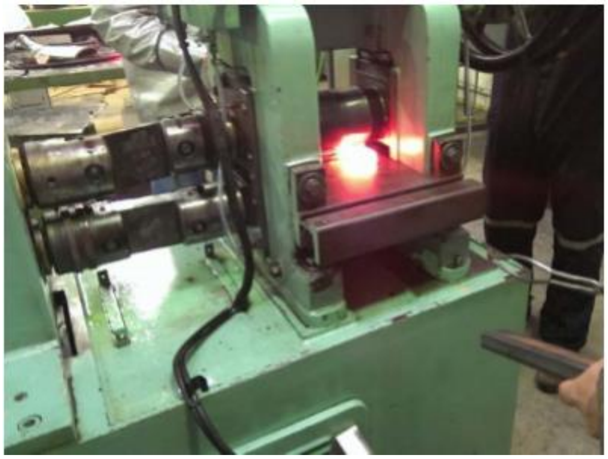

Figure 4. Hot rolling at 1200°C.

Figure 5. Rolled sample (60% section reduction).

followed by air-cooling.

- Austenisation heat treatment for 0.5 h at 1100°C followed by air-cooling.
- Tempering for 2 h at 780°C with subsequent air-cooling.

2.3 Microstructure investigation

The microstructure of the alloys was analysed in the initial state (after tempering at 780 °C/2h) by light optical microscopy (LM) and transmission electron microscopy (TEM). LM specimens were prepared by mechanical grinding (down to 1.200 SiC grade paper), followed by mechanical polishing with 6, 3 and 1µm diamond paste. The samples were etched using Vilella's reagent (1 vol% picric acid and 5 vol% concentrated hydrochloric acid in ethanol). Optical micrographs were taken using an Olympus GX51 microscope equipped with a Micrometrics 590CU CCD camera. The carbon extracted replication method was used to prepare the TEM specimens [15].

The samples were prepared by mechanical grinding (down to 1.200 grade paper), followed by mechanical polishing with 6, 3 and 1 µm diamond paste. A chemical etching of polished surfaces was performed with Vilella's reagent for about 15 seconds. A carbon film is deposited onto the specimen by carbon evaporation. Thereafter, the film is cut into pieces and the samples are dissolved in Vilella's reagent, leaving the carbon extraction replica in the solution. The replicas are cleaned with ethanol and caught on small copper grids. Carbon extracted replicas provide more accurate measurements of the chemical composition and crystallographic structure of the precipitates. In addition, this method minimised the magnetic aberrations due to the dissolution of the ferritic matrix [15] The TEM images were taken in a JEOLJEM 1200 EX II operating at 120 kV microscope.

3. Results and discussion

3.1 Alloy design

The main objective related to the design of new 10-12%Cr Martensitic/Feritic steels is to achieve high creep resistance, ideally 100.000 hours at temperatures up to 650 °C, with a pressure about 100 MPa. To achieve this objective the chemical composition of the alloys is very important, because this is directly related to the formation of stable phases and precipitates, which block the movement of dislocations, grain boundaries and sub-grain boundaries. Additionally, the formation of stable precipitates may improve the creep resistance of the steels extending their service life. In the following, the main precipitates required in the microstructure are described:

- **$M_{23}C_6$:** Cr rich precipitates which provides high mechanical stability and the basic creep resistance to the alloys. The formation of this phase must be controlled in order to avoid the depletion of Cr of the matrix, which decreases the corrosion resistance to the steels [16].
- **MX:** The M denotes a metal which forms carbides and/or carbonitrides (V, Nb, Ti, etc.) and the X denotes C and/or N. These precipitates provide

additional creep resistance, owing to its small size, even distribution and high stability related to its slow coarsening kinetics. They increase creep strength by pinning free dislocations and sub-grain boundaries [17].

- **Laves phase:** This is an intermetallic phase of the type (Fe,Cr)$_2$(W,Mo) which may precipitate in W and Mo containing steels. Often the laves phase nucleates and precipitates during service, after several hundred hours of exposure at high temperature and pressure. The coarsening rate is slow, thus can be used to improve the creep resistance by blocking grain and sub grain boundaries [18], if the nucleation sites and the particle size are controlled.

Two lines of study were defined to design the alloys. The first considers the additions of V and Nb together with C and N, in order to form MX and W to promote the formation of Laves phase. Although has been informed that the V and Nb together with Cr and N additions drives the precipitation of Zphase, detrimental carbonitride which decreases the creep strength, several studies had reported that steels with restricted Cr content do not suffer from abundant formation of Z-phase after long-term creep [17], due to the slow kinetics of the Z-phase formation. The second line of investigation considers additions of V, Nb and Ti together with C and N. The Ti combined with C and N promotes the precipitation of Ti-MX. These particles have an extremely high stability and thus a high potential for strengthening the alloys. Additionally, Ti-MX particles have a higher stability than the Z-phase at 650°C; therefore the formation of Z-phase is avoided with the Ti additions. Additions of Mo, W and Ni, aims to obtain a finer and evenly distributed Laves phase in comparison to the alloy which contains only W [19]. Considering the metallurgical principles explained above, a study to determine the effect of several alloying elements was carried out by the development of phase diagrams (modelled with ThermoCalc). ThermoCalc software allows equilibrium calculations, phase stability evaluation and determination of heat treatment temperatures for multicomponent systems. Upon modelling, the time and costs of trialand-error of conventional alloy development can be reduced. All calculations were carried out with the ThermoCalc database TCFe$_7$ (last version) [12]. This database includes a new more accurate definition of the Laves and the Z phase.

- **Alloy design 10.5CrWVNb:** The Cr content provide high corrosion and oxidation resistance required to work at temperatures up to 650°C. Furthermore, the Cr promotes the formation of $M_{23}C_6$ carbides, the most commune precipitate in these steels. The $M_{23}C_6$ confer the basic creep strength to the steels by the stabilisation of the microstructure. These carbides block the grain and sub-grain boundaries, reducing the microstructural degradation improving the creep strength [16].

Fig. 6 shows a phase diagram which varies the Cr content. The Cr addition was fixed between 10 and 11%, in order to increase the corrosion resistance. Higher amount of Cr promote the formation of δferrite (see Fig. 6), detrimental phase which reduce the creep strength of the steels. In addition, several authors have demonstrated that high Cr contents (around 12%) increase the precipitation driving force of Z-phase. The Z-phase causes the dissolution of MX carbonitrides, which are beneficial to the creep strength. Hence progressive Z-phase precipitation causes breakdown in creep strength [20]. Fig. 7 shows a phase diagram where the Co content varies within a base alloy. Co is used in order to stabilise the austenitic field, showing a high solubility in the ferrite and low solubility in the precipitates, mainly remaining in the matrix as solid solution. Co also raises the Ms and the Curie temperature and it is expected to slow down diffusion processes, reducing the coarsening of the precipitates, which increases creep strength [21].

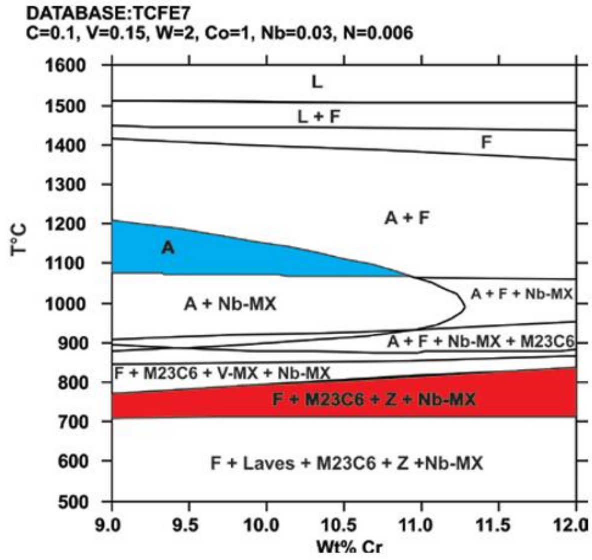

Figure 6. Phase diagram built by ThermoCalc varying %Cr (A = Austenite, F = Ferrite), 10.5CrWVNb.

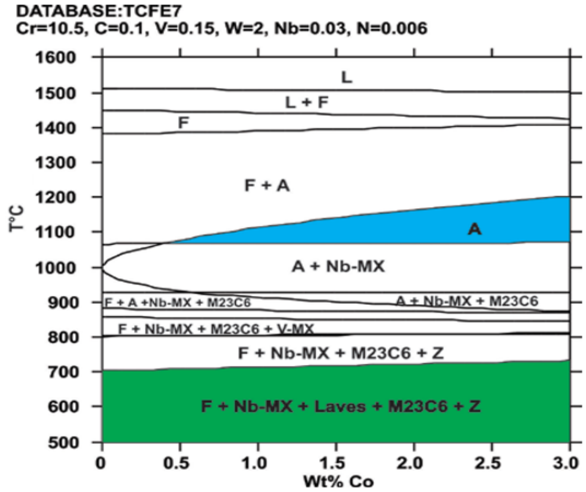

Figure 7. Phase diagram built by Thermo-Calc varying %Co (A = Austenite, F = Ferrite), 10.5CrWVNb.

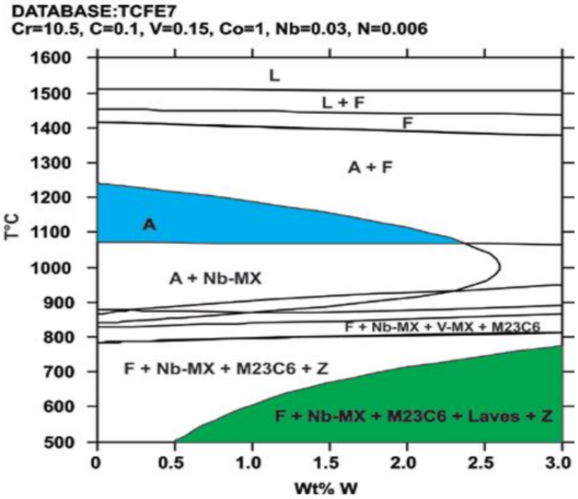

Figure 8. Phase diagram built by ThermoCalc varying %W (A = Austenite, F = Ferrite), 10.5CrWVNb.

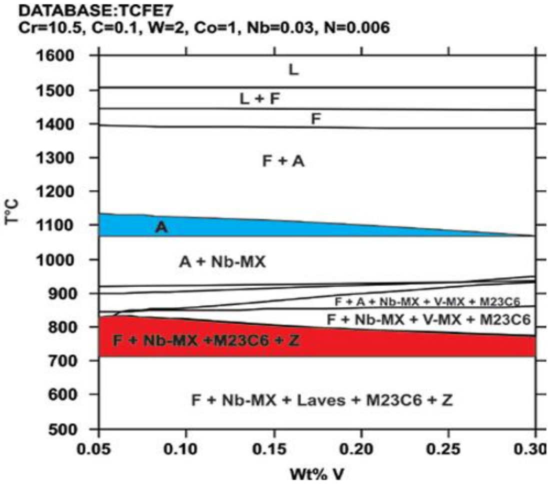

Figure 9. Phase diagram built by ThermoCalc varying %V (A = Austenite, F = Ferrite), 10.5CrWVNb.

Fig. 7 shows a phase diagram where the Co content varies within a base alloy. Co is used in order to stabilise the austenitic field, showing a high solubility in the ferrite and low solubility in the precipitates, mainly remaining in the matrix as solid solution. Co also raises the Ms and the Curie temperature and it is expected to slow down diffusion processes, reducing the coarsening of the precipitates, which increases creep strength [21]. The figure 7 shows that with 1% Co is enough to avoid the precipitation of δ-ferrite. Higher Co content would not be detrimental to the alloy, but the Co addition is restricted till 2% considering the high cost of this metal.

Fig. 8 shows a phase diagram where the W content varies within a base alloy. W is well known to increase the high temperature strength via solid solution hardening [22]. Additionally, it has been reported that increased W concentrations, may reduce the coarsening rate of $M_{23}C_6$ carbides, thus delaying the degradation of the lath martensitic microstructure [23]. W is a strong Laves phase former, this intermetallic is used to delay even more the microstructure degradation, due to Laves phase presents a slow coarsening kinetic comparing to the $M_{23}C_6$. As was mentioned above, Laves phase nucleates and precipitates during service, after several hundred hours of exposure at high temperature and pressure when the $M_{23}C_6$ carbides become less effective against the creep [18]. The W content was fixed between 1.5 and 2.2%. The lower limit 1.5% W, is selected to ensure precipitation of the Laves phase, while the upper limit about 2.2% W consider to achieve a fully austenitic field, avoiding the formation of δ-ferrite.

Fig. 9 shows the effect of V in a base alloy. V addition promotes the precipitation of V carbonitrides, highly desirable to improve the creep strength. V content is limited to 0.15%, because further additions of this element leaves a very narrow range to perform the austenisation heat treatment (V promotes the formation of δ-ferrite). In addition, it has been demonstrated that higher content of V increases the precipitation driving force of Z-phase [7]. However, the Z-phase formation from V-MX takes place after several hundred hours under service conditions [8]. One objective of this work is to study the feasibility of produce 10.5% Cr alloys without high amounts of Z-phase after long-term creep, in order to avoid a significantly breakdown on the creep strength.

Nb addition promotes the precipitation of Nb-MX. The Nb carbonitrides increase the creep strength by pinning free dislocations and sub-grain boundaries [24]. However, the Nb-MX particles present a high precipitation temperature, which increases as the Nb content enlarge (Fig. 10). An excess of Nb would promote the formation of δ-ferrite, which decreases the creep strength. Therefore, the Nb content was determined between 0.02 and 0.04%.

The N and C additions are fundamental for the precipitation of carbides and carbonitrides. Moreover, B stabilise the $M_{23}C_6$ by using the interstitial spaces, which reduces the diffusion and the coarsening kinetics. The N and B have a close relation, N and B additions should be carefully controlled because excess of these elements promote the formation of BN, detrimental nitride which decrease the mechanical properties, weldability and the creep strength [25]. The N content was fixed between 0.003 and 0.01%, while the B content was considered with a 0.015% as maximum content.

Fig. 11 shows a phase diagram varying the C content. It can be observed that with 0.1%C and temperatures between 1055 and 1110°C a fully austenitic field is obtained. Whiting this austenitic field, the austenisation heat treatment must be carried out. Therefore, the C content was fixed between 0.1 and 0.15%C. The table 1 shows the chemical composition range designed for alloy 10.5CrWVNb.

Alloy design 10.5CrTiMo: Based on the phase diagrams modelled for the alloy 10.5CrWVNb and metallurgical principles described above, the Cr content for the alloy 10.5CrTiMo was fixed between 10 and 11%, V content was fixed between 0.1 and 0.2%, N between 0.003 and 0.006% and B content was considered with a 0.015% as maximum content. In order to obtain a finer and uniform distribution of Laves phase, Mo, W and Ni are added to the alloy. Mo content was fixed between 1 and 2%, Ni content should not exceeds 0.12% otherwise would decrease the creep strength [2]. The W content was set between 0.5 and 1.5% depending to the Mo content. The combination of Mo and W should not exceed the 2.2%, otherwise will promote the formation of δ-ferrite.

The Ti content was fixed at 0.03% to drive the formation of Ti-MX. The Ti carbonitrides are more stable than the Z-phase at 650°C (see Fig. 12 and 13), thus they effectively avoid the precipitation of Z-phase. The Ti precipitates have a very high stability and they showed a very slow coarsening rate [26]. However, the phase diagram in Fig. 12, indicates that the precipitation of Ti-MX start already in the liquid (around 1450 °C), even for small additions of Ti, and there is nearly no change in the amount of the phase with decreasing temperature. Therefore, it seemed to be difficult to control the size and distribution of the Ti-MX in the microstructure.

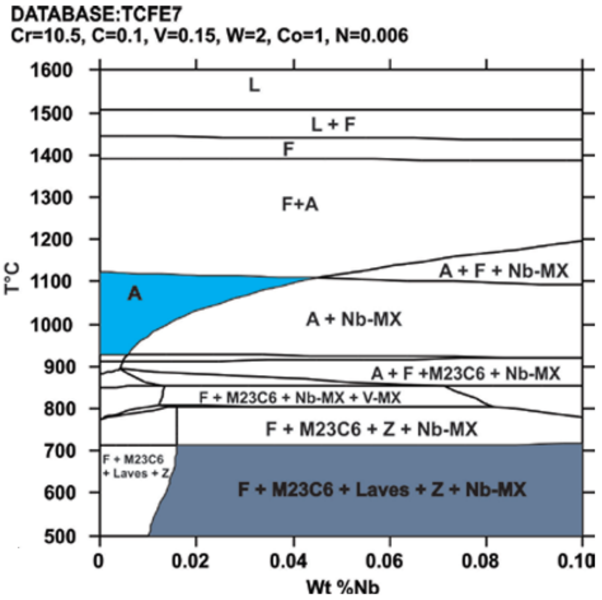

Figure 10. Phase diagram built by ThermoCalc varying %Nb (A = Austenite, F = Ferrite), 10.5CrWVNb.

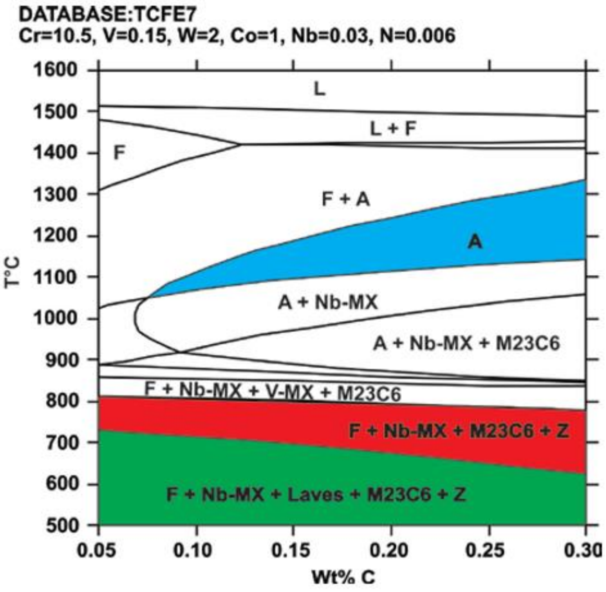

Figure 11. Phase diagram built by ThermoCalc varying %C (A = Austenite, F = Ferrite), 10.5CrWVNb.

Table 1. Nominal chemical composition range alloy 10.5CrWVNb.

	C	Si	Mn	Co	B	Cr	W	Mo	V	N	Ti	Ni	Nb	Fe
10.5CrTiMo	0,10 – 0,15	0,35 – 0,45	0,35 – 0,45	1,50 - 2,5	0,005 – 0,015	10,0 – 11,0	0,50 – 1.50	1,00 – 2,00	0,10 – 0,20	0,003 – 0,006	0,01 – 0,03	0,05 - 0,12	0,01 – 0,03	Bal .

Table 2. Nominal chemical composition range alloy 10.5CrTiMo.

	C	Si	Mn	Co	B	Cr	W	Mo	V	N	Ti	Ni	Nb	Fe
10.5CrTiMo	0,10 – 0,15	0,35 – 0,45	0,35 – 0,45	1,50 - 2,5	0,005 – 0,015	10,0 – 11,0	0,50 – 1.50	1,00 – 2,00	0,10 – 0,20	0,003 – 0,006	0,01 – 0,03	0,05 - 0,12	0,01 – 0,03	Bal .

Table 3. Chemical composition of 10.5CrWVNb and 10.5CrTiMo (by optical emission spectrometer).

	C	Si	Mn	Co	B	Cr	W	Mo	V	N	Ti	Ni	Nb	Fe
10.5CrWVNb	0.09	0.38	0.42	0.95	0.012	10.3	2	-	0.14	0.005	-	-	0.027	Bal
10.5CrTiMo	0.04	0.20	0.1	2.0	0.001	10.5	1	1.6	0.14	0.01	0,005	0.1	0.02	Bal

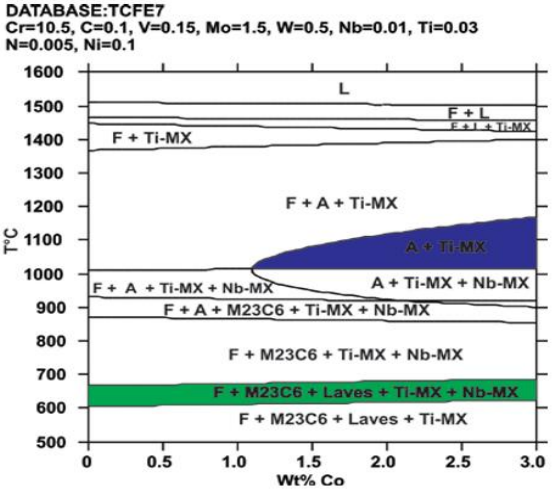

Figure 12. Phase diagram built by ThermoCalc varying %Co (A = Austenite, F = Ferrite), 10.5CrTiMo.

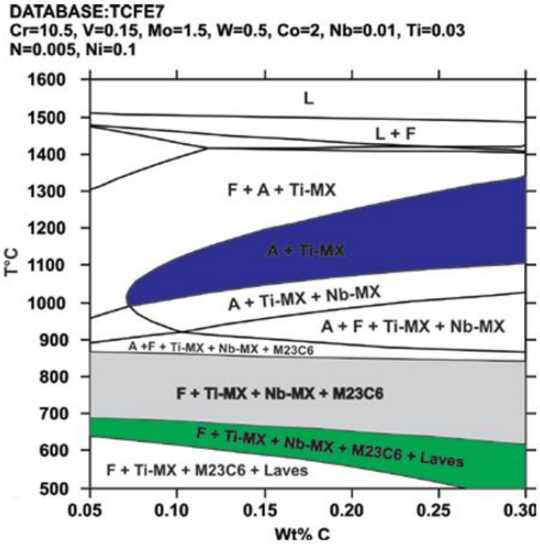

Figure 13. Phase diagram built by ThermoCalc varying %C (A = Austenite, F = Ferrite), 10.5CrTiMo.

Due to the higher addition of ferrite stabilising elements (Ti, W, Nb, V and Mo), the Co content should be increased to about 1.5%, in order to avoid the formation of δ-ferrite, as is shown in Fig. 12. The maximum Co content is limited to 2.5% considering the high cost of Co.

Fig. 13 shows a phase diagram varying the C content. With C between 0.1 and 0.15% it is possible to observe a phase field containing austenite and Ti-MX above 1000 °C. The austenisation heat treatment should be performed at the highest temperature possible, in order to dissolve as much Ti-MX, according to the diagram between 1000 and 1100 °C.

3.2 Chemical composition and microestructural investigation of produced alloys

Based on the thermodynamic calculations the two alloys were produced as was detailed in the experimental procedure. The temperatures for the different heat treatments (autenisation and tempering) were determined by the modelled phase diagram from each designed alloy. The chemical composition is shown in the table 3. In order to obtain the designed alloys composition, two mass balances were performed to charge the furnace with different scrap material, 99% Cr and ferroalloying elements.

The table 3 shows the experimental chemical composition of alloy 10.5CrWVNb that was very accurate with the designed alloy. The steel 10.5CrWVNb presented a martensitic/ferritic matrix with high density of internal interfaces, such as prior austenite grain boundaries (PAGB, see Fig.

14A and 14B), block, lath and sub-grain boundaries and high dislocation density. The high dislocation density is produced when martensite forms during air-cooling after the austenisation heat treatment. During tempering the precipitation of solute atoms occurs, as well as recovery of the dislocation cell structure resulting in a sub-grain structure [27]. The Fig. 14A shows a very few amount of δ-ferrite, in agreement to the thermodynamic calculations. Fig 14C and 14D shown carbon extracted replica images, where is possible to observe the different precipitates, mainly $M_{23}C_6$ carbides which are uniformly distributed. Due to the TEM limitations, was not possible to identify the MX particles. However in a further study they will be identify to corroborate the thermodynamic calculations. The experimental chemical composition of alloy 10.5CrTiMo is shown in table 3. As is possible to observe, the chemical results differed from the design composition. The C content for 10.5CrTiMo was too low (0.04%) this leads the formation of high amount of δ-ferrite, that is detrimental for the creep strength. Fig 15A shows very big ferritic grains, with few smaller martensitic/ferritic grains. Fig. 15B shows small precipitates with sharp edges, which may correspond to Ti-MX. This must be corroborated with further microstructure characterisation. The Laves phase was not found upon the microstructure, in agreement with the reported by the literature [18]. Laves phase is expected to form after several hundred hours under service conditions.

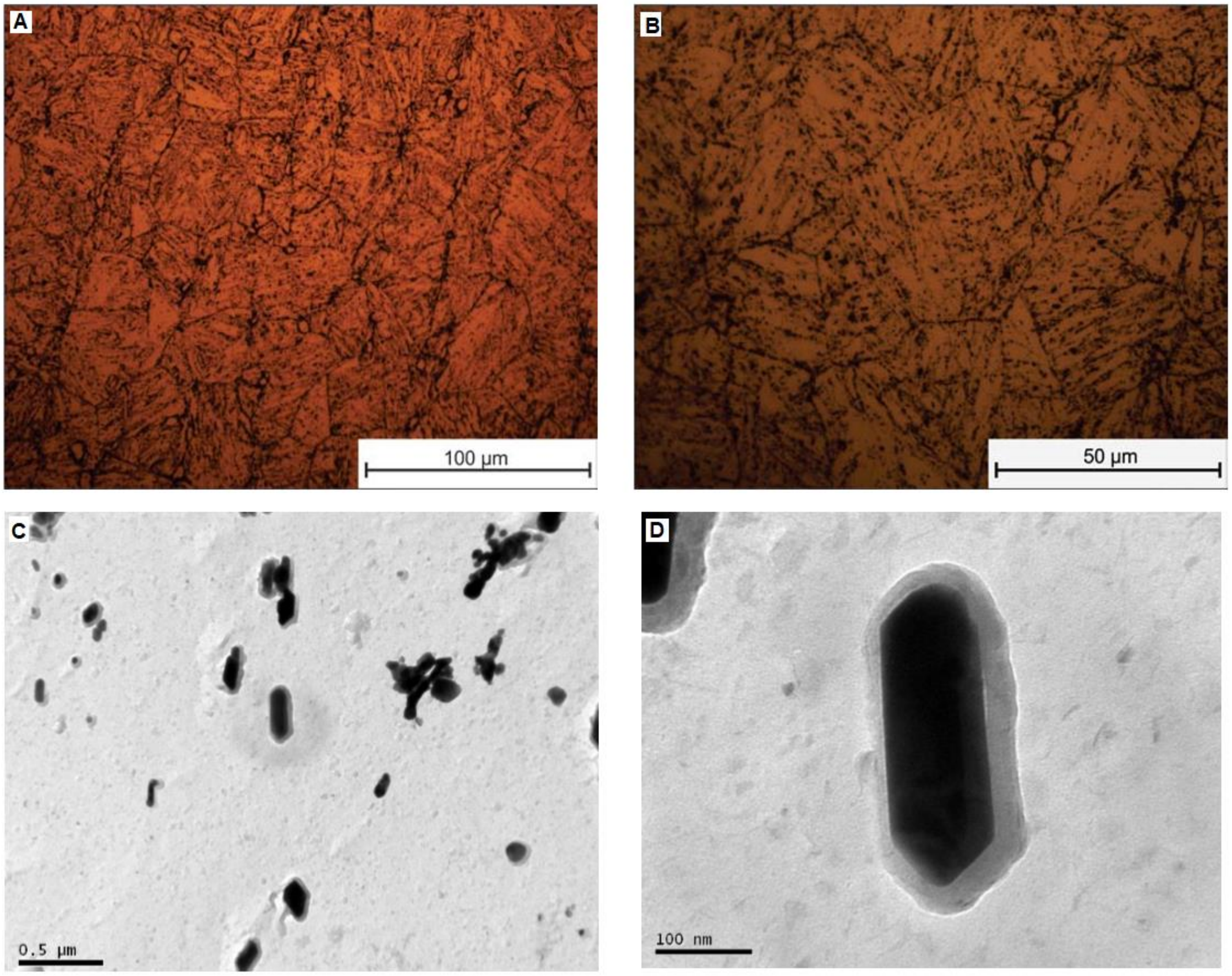

Figure 14. (A) Microstructure alloy 10.5CrWVNb showing a martensitic/ferritic matrix and secondary phases, (B) Microstructure alloy 10.5CrWVNb, showing the PAGB, (C) Carbon replica image from alloy 10.5CrWVNb, showing mainly M23C6 carbides and (D) Carbon replica image from alloy 10.5CrWVNb. Zoom to M23C6 carbide.

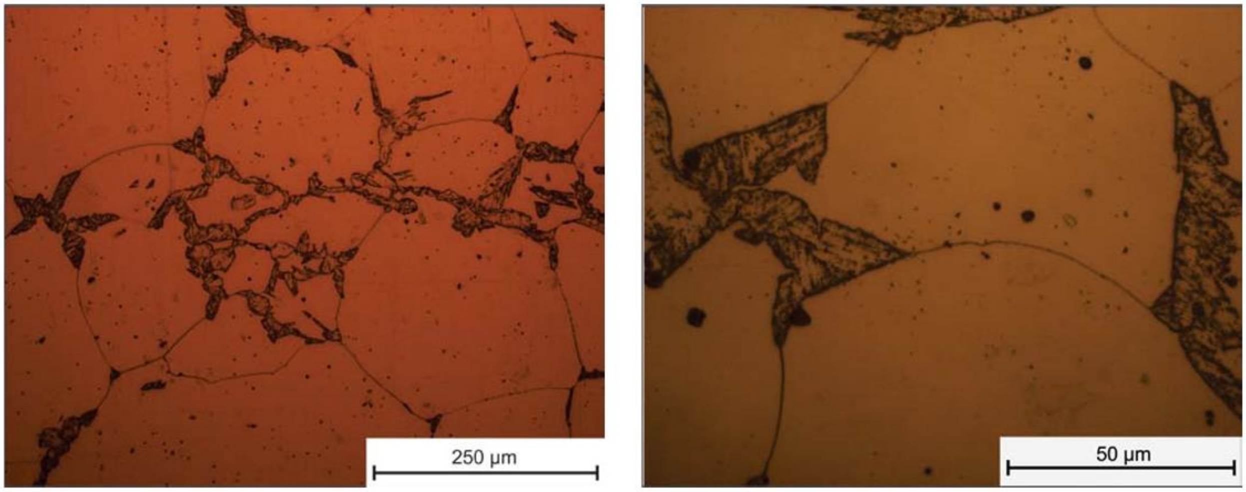

Figure 15. (A) Microstructure alloy 10.5CrTiMo showing a ferritic matrix, left, and (B) Microstructure 10.5CrTiMo, showing small precipitates, right.

4. Conclusion

In the present work two 10.5%Cr steels were design and produced. A detailed study regarding the effect of the alloying elements and the selection of the precipitates, which enhance the creep resistant properties was carried out considering metallurgical principles and thermodynamic modelling. The conclusions of the study are summarised as follows:

- ThermoCalc calculations showed to be a reliable tool for alloy development. The heat treatment temperatures were defined based on the modelled phase diagrams.
- ThermoCalc calculation showed that in the alloy 10.5CrWVNb Z-phase is the most stable carbonitride at 650°C. For the alloy 10.5CrTiMo the modelled phase diagrams showed that the Ti-based MX particles have a higher stability then Z-phase. Therefore, The Ti-MX are promising precipitates for improve the creep strengthening, avoiding the precipitation of Z-phase.
- The steel 10.5CrWVNb presented a martensitic/ ferritic matrix with high density of internal interfaces and showed high amount of precipitates, mainly M23C6, uniformly distributed within the matrix.
- The steel 10.5CrTiMo shows very big ferritic grains, with few smaller grains with a martensitic/ferritic structure due to the low carbon content, also shows small precipitates with sharp edges, which may correspond to Ti-MX.
- The Laves phase was not found upon the microstructure in both steels, this is in agreement with the reported by previous investigations carried out by the authors.

Acknowledgements

Dr. D. Rojas thanks the collaboration of the “Universidad de Concepción” and gratefully acknowledges the financial support from “Proyecto FONDECYT de iniciación N°11110098, Gobierno de Chile”

Conflict of interts

The authors declare no conflict of interest of any kind in relation to the publication.

References

[1] R. Blum, R. W. Vanstone, Proc. 8th Liege Conf. Materials for Advanced Power Engineering, Liege, Belgium (2006), pp. 41-60.

[2] F. Abe, T.-U. Kern, R. Viswanathan, “Creep-resistant steels”, Woodhead Publishing, CRC Press Cambridge, England (2008).

[3] G. Eggeler, N. Nilsvang, B. Ilschner, Steel Res. 58 (1987) 97-103.

[4] J. Hald, Proc. 9th Liege Conf. Materials for Advanced Power Engineering, Liege, Belgium (2010), pp. 55-66.

[5] S. Straub, T. Hennige, P. Polcik, and W. Blum, Steel Res. 66 (1995) 394-401.

[6] C. Berger, A. Scholz, Y. Wang, K.-H. Mayer, Z. Metallkd. 96 (2005) 668-674.

[7] L. Cipolla, H. K. Danilesen, D. Venditti, P. E. Di Nunzio, J. Hald, M. A. J. Somers, Acta Mater. 58 (2010) 669-679.

[8] H. K. Danielsen, J. Hald, Energy Mater. 1 (2006) 49-57.

[9] A. Strang, V. Vodarek, Mater. Sci. Technol. 12 (1996) 552-556.

[10] A. Kimura, R. Kasada, A. Kohyama, H. Tanigawa, T. Hirose, K. Shiba, S. Jitsukawa, S. Ohtsuka, S. Ukai, M. A. Sokolov, R. L. Klueh, T. Yamamoto, G. R. Odette, J. Nucl. Mater. 367 (2007) 60-67.

[11] Y. Wanga, K.-H. Mayer, A. Scholz, C. Berger, H. Chilukuru, K. Durst,W. Blum, Mater. Sci. Eng. A 510-511 (2009) 180-184.

[12] TCFE7: TCS Steel and Fe-alloys DataBase provided by Thermocalc soft AB. http://www.thermocalc.com/ TCDATA.htm (2013).

[13] D. Rojas, J. Garcia, O. Prat, C. Carrasco, G. Sauthoff, A.R. Kaysser-Pyzalla, Mater. Sci. Eng. A 527 (2010) 3864-3876.

[14] D. Rojas, J. García, O. Prat, G. Sauthoff, A. R. Kaysser-Pyzalla, Mater. Sci. Eng. A 528 (2011) 51645176.

[15] D. R. G. Mitchell, S. Sulaiman, Mater. Charact. 56 (2006) 49-58.

[16] J. Hald, L. Korcakova, ISIJ int. 43 (2003) 420-427.

[17] M. Taneike, K. Sawada, F. Abe, Metall. Mate. Trans. A 35A (2004) 1255-1262.

[18] O. Prat, J. Garcia, D. Rojas, C. Carrasco, G. Inden, Acta Mater. 58 (2010) 6142-6153.

[19] F. Abe, T. Horiuchi, M. Taneike, K. Sawada, Mater. Sci. Eng. A 378 (2004) 299-303.

[20] L. Cipolla. H. K. Danilesen. D. Venditti, P. E. Di Nunzio, J. Hald, M. A. J. Somers, Acta Mater. 58 (2010) 669-679.

[21] L. Helis, Y. Toda, T. Hara, H. Miyazaki, F. Abe, Mater. Sci. Eng. A 510-511 (2009) 88-94.

[22] F. Abe, Mater. Sci. Eng. A 387-389 (2004) 565-569.

[23] K. Sawada, M Takeda, K. Murayama, R. Ishii, M. Yamada, Y. Nygae, R. Komine, Metall. Mater. Trans. A 267 (1999)19-25.

[24] T. Fujita, N. Takahashi, T. Iron Steel Jpn. 18 (1979) 269-278.

[25] F. Abe, Curr. Opin. Solid St. M. 8 (2004) 305-311.

[26] V. Knezevic, J. Balun, G. Sauthoff, G. Inden, A. Schneider, Mater. Sci. Eng. A 477 (2008) 334-343.

[27] D. Rojas, J. Garcia, O. Prat, L. Agudo, C. Carrasco, G. Sauthoff, A.R. Kaysser-Pyzalla, Mater. Sci. Eng. A 528 (2011) 1372-1381.